# Characterization of endogenous human Argonautes and their miRNA partners in RNA silencing

Asuka Azuma-Mukai[†], Hideo Oguri[‡], Toutai Mituyama[§], Zhi Rong Qian[†], Kiyoshi Asai[§¶], Haruhiko Siomi[†‖], and Mikiko C. Siomi[†‖††‡‡]

[†]Institute for Genome Research, University of Tokushima, Tokushima 770-8503, Japan; [‡]First Institute of New Drug Discovery, Otsuka Pharmaceutical Co., Ltd., Tokushima 771-0192, Japan; [§]Computational Biology Research Center, National Institute of Advanced Industrial Science and Technology (AIST), Tokyo 135-00664, Japan; [¶]Graduate School of Frontier Science, University of Tokyo, Chiba 277-8561, Japan; [††]Japan Science and Technology Agency, Core Research for Evolutional Science and Technology, Saitama 332-0012, Japan; and [‖]Keio University School of Medicine, Tokyo 160-8582, Japan

Edited by Michael Rosbash, Brandeis University, Waltham, MA, and approved March 21, 2008 (received for review January 11, 2008)

**Small RNAs triggering RNA silencing are loaded onto Argonautes and then sequence-specifically guide them to target transcripts. Epitope-tagged human Argonautes (hAgo1, hAgo2, hAgo3, and hAgo4) are associated with siRNAs and miRNAs, but only epitope-tagged hAgo2 has been shown to have Slicer activity. Contrarily, how endogenous hAgos behave with respect to small RNA association and target RNA destruction has remained unclear. Here, we produced monoclonal antibodies for individual hAgos. High-throughput pyrosequencing revealed that immunopurified endogenous hAgo2 and hAgo3 associated mostly with miRNAs. Endogenous hAgo3 did not show Slicer function but localized in P-bodies, suggesting that hAgo3 endogenously expressed is, like hAgo2, involved in the miRNA pathway but antagonizes the RNAi activity of hAgo2. Sequence variations of miRNAs were found at both 5′ and 3′ ends, suggesting that multiple mature miRNAs containing different ''seed'' sequences can arise from one miRNA precursor. The hAgo antibodies we raised are valuable tools for ascertaining the functional behavior of endogenous Argonautes and miRNAs in RNA silencing.**

Jurkat | siRNAs | Slicer

RNA silencing is an evolutionarily conserved physiological process regulating gene expression (1). RNA interference (RNAi), the prototype of RNA silencing, down-regulates gene expression by cleaving target mRNAs in a sequence-dependent manner (2). A molecule that renders sequence-specificity is the short interfering RNA (siRNA) of 21- to 23-nt length. MicroRNAs (miRNAs) are a large set of endogenous small RNAs (21–23 nt long) encoded in the genome of a variety of organisms (3). miRNA functions in RNA silencing by regulating the expression of target genes by inhibiting translation or destructing mRNAs (3, 4). The miRNA target genes identified to date have mostly been involved in vital biological processes such as development, apoptosis, neural patterning, and viral infection. The origins of siRNAs and miRNAs differ from each other, but both are processed from a longer double-stranded RNA precursor by RNase III domain-containing Dicer and loaded onto a member of the Argonaute family of proteins (2).

Members of the Argonaute family are defined by the presence of the PAZ and PIWI domains (5). The numbers of Argonaute members vary from species to species. In humans, the Argonaute family has eight members, four of which (AGO subfamily members; hAgo1–hAgo4) are expressed in numerous tissues and cell types (5). Although comprehensive analysis remains to be done, expressions of other members of the Argonaute family in humans (PIWI subfamily members; Hiwi1, Hiwi2, Hiwi3, and Hili) appear to be restricted to germ lines. Recent studies on rodents, fish, and flies have revealed that Argonautes expressed only in germ lines (PIWI subfamily members) are associated with piRNAs (Piwi-interacting small RNAs), a subset of small RNAs exclusively expressed in germ lines (6). Unlike miRNAs, piRNAs are 24 to 31 nt long and derived from discrete piRNA loci of chromosomes in a Dicer-independent manner (7). piRNAs are necessary for gametogenesis in organisms. In particular, it has been shown that in flies, piRNAs function in silencing retrotransposons to preserve DNA integrity in germline cells (6).

Much of the evidence obtained to date supports the concept that ubiquitously expressed Argonautes (namely AGO subfamily members) function in RNA silencing through specific association with siRNAs and miRNAs (5). It has been reported that the immunoprecipitates of anti-hAgo2 contain miRNAs (8, 9); however, if the antibody specifically recognized hAgo2 or cross-reacted with other hAgos was, at that time, an unanswered issue. Later, biochemical analysis of all hAgos in respect to small RNA association was performed with epitope-tagged hAgos expressed in mammalian cells, revealing that both miRNAs and siRNAs are indiscriminately associated with hAgo1 through hAgo4 containing miRNPs (10, 11). It has also been demonstrated that Slicer activity is exclusively associated with hAgo2 (11, 12). Disruption of the mouse Ago2 (mAgo2) gene produced an embryonic-lethal phenotype (10), suggesting that Argonautes are not redundant and might be biologically specialized.

Recently, biochemical approaches were established for predicting miRNA targets in human cells (12). In that study, hAgo1 and hAgo2 exogenously expressed in HEK 293 cells were immunopurified with specific antibodies against hAgo1 and hAgo2. cDNA libraries were then generated from the mRNA pools extracted from the immunoprecipitates. Identification of cDNA clones in the libraries revealed that only a limited number of mRNA overlap between hAgo1 and hAgo2. It was suggested that many miRNA targets might be specific to one Ago protein.

As indicated above, functional analyses of hAgos have so far been performed by using epitope-tagged, exogenously expressed Argonautes. However, how endogenous hAgos behave in regard to small RNA association and target RNA destruction has not been determined. To address these questions, we produced monoclonal antibodies against each of the hAgos and identified small RNAs associated with endogenous hAgo2 and hAgo3. High-throughput pyrosequencing revealed that hAgo2 and hAgo3 immunopurified from Jurkat cells are mostly associated with miRNAs, which in the hAgo2 and hAgo3 libraries are largely overlapped with only a few miRNAs detected discrimi-

Author contributions: A.A.-M., H.O., T.M., K.A., H.S., and M.C.S. designed research; A.A.-M., H.O., T.M., and Z.R.Q. performed research; A.A.-M., H.O., T.M., and Z.R.Q. contributed new reagents/analytic tools; A.A.-M., H.O., T.M., Z.R.Q., K.A., H.S., and M.C.S. analyzed data; and H.S. and M.C.S. wrote the paper.

The authors declare no conflict of interest.

This article is a PNAS Direct Submission.

Data deposition: The miRNAs found in this study [hsa-mir-1537, hsa-mir-1538, hsa-mir-1539, hsa-mir-1284, and hsa-mir-103-1-as (chr5)/hsa-mir-103-2-as (chr20)] have been deposited in miRBase (http://microrna.sanger.ac.uk).

‡‡To whom correspondence should be addressed. E-mail: siomim@sc.itc.keio.ac.jp.

This article contains supporting information online at www.pnas.org/cgi/content/full/0800334105/DCSupplemental.

nately. Sequence variations in miRNAs were observed at both 5′ and 3′ ends, raising the possibility that miRNAs containing different "seed" sequences are multiply produced *in vivo* from one precursor sequence. Strong accumulation of endogenous hAgo2 and hAgo3 into P-bodies further supports hAgo3 involvement in miRNA-mediated RNA silencing pathways. However, endogenous hAgo3 associated with miRNA and siRNA showed little or no Slicer activity *in vitro*, suggesting that hAgo3 antagonizes RNAi activity in cells. The antibodies we raised against individual hAgos are valuable tools to reveal the functional behavior of endogenous Argonautes and their miRNA partners in RNA silencing mechanisms.

## Results

**Monoclonal Antibodies for Individual Endogenous hAgos.** It has been previously reported that hAgo1, hAgo2, hAgo3, and hAgo4 associate with both siRNAs and miRNAs (10, 11). However, all such analyses have been performed by using exogenously expressed, epitope-tagged hAgos in mammalian cells (10, 11). By contrast, how endogenous hAgos behave in regard to small RNA association has remained unelucidated. This prompted us to produce antibodies specifically recognizing individual hAgos. We expected that these would be useful for ascertaining endogenous hAgo functions in RNA silencing. As antigens to immunize mice, we used N-terminal regions of hAgos, because the regions show relatively lower similarities compared with others, including the highly conserved PAZ and PIWI domains [supporting information (SI) Fig. S1]. Antibody specificity was determined by Western blot analysis on the peptides used for immunizing mice. This indicated that monoclonal antibodies specific for individual hAgos were successfully obtained (Fig. S2). Western blot analysis data on human cell lysates with the antibodies is shown in Fig. S2*F*.

We assessed whether anti-hAgos work for immunoprecipitation. It has been shown that Flag-tagged-hAgo1 copurifies with eGFP-hAgo2 from HEK 293 cells (13). In our experiments, to avoid such undesired protein–protein interactions, a strong zwitterionic detergent, Empigen, was used. Even under harsh conditions, hAgo2 and hAgo3 were efficiently immunoprecipitated from Jurkat cells (Fig. 1*A*). Western blot analysis determined that the protein bands indicated with arrowheads on the silver-stained gel (Fig. 1*A*) correspond to hAgo2 (green) and hAgo3 (red) (Fig. 1 *B* and *C*). No other hAgos were detected in the hAgo2 and hAgo3 immunoprecipitates (Fig. S3). Anti-hAgo1 was inefficient for immunoprecipitation (data not shown). Anti-hAgo4 immunoprecipitated hAgo4 (blue arrowhead in Fig. 1*A*), but it also reacted to other proteins (single and double asterisks in Fig. 1*A* and Fig. S3*C*). Mass spectrometric analysis identified the protein migrating at nearly 120 kDa (double asterisks in Fig. 1*A* and Fig. S3*C*) as the E1B-55kDa-associated protein (accession no. CAA07548), a cellular protein implicated in the nucleocytoplasmic transport of adenovirus and cellular mRNAs (14); however, no implication in RNA silencing has yet been reported.

Anti-hAgo2 and -hAgo3 were also useful for immunostaining; we found that both hAgo2 and hAgo3 localized in P-bodies (processing bodies) (Fig. 2), the cytoplasmic foci where miRNA targets are accumulated as a consequence of translational repression (15, 16). P-bodies, where DCP1a, a factor functioning in mRNA decay in the bodies (17), resides, were mostly costained with anti-hAgo2 or anti-hAgo3. hAgo2 and hAgo3 are unlikely to be sorted into different sets of P-bodies.

**Small RNAs Associated with Endogenous hAgo2 and hAgo3.** Small RNAs associated with endogenous hAgo2 and hAgo3 in mammalian cells are as yet undetermined. In this study, RNAs were purified from immunopurified endogenous hAgo2 and hAgo3 (Fig. 1*A*) and visualized by $^{32}$P-labeling. Both proteins were revealed to associate with small RNAs ranging from 21 to 23 nt (Fig. 3*A*). It was noted that the exposure time for hAgo3 small RNAs was approximately three times longer than that of hAgo2 small RNAs, indicating that the amount of hAgo3 small RNAs

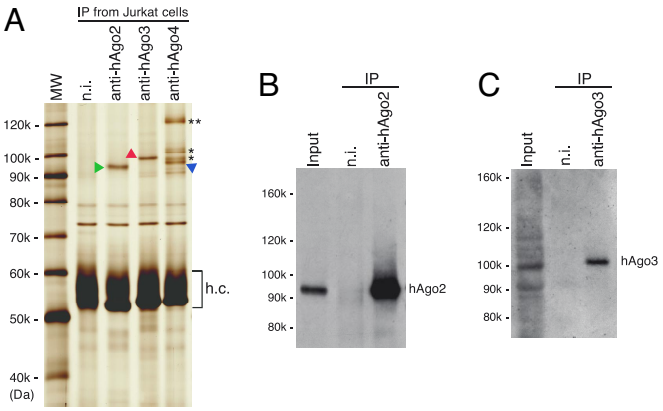


**Fig. 1.** Characterization of immunoprecipitates with anti-hAgo2, -hAgo3, and -hAgo4 antibodies from Jurkat cells. (*A*) Jurkat cell lysates prepared with a cell lysis buffer containing Empigen, and immunoprecipitation performed by using anti-hAgo2, -hAgo3, and -hAgo4 antibodies. Protein components in the immunoprecipitates were stained with silver. Protein bands indicated with arrowheads in green, red, and blue are hAgo2, hAgo3, and hAgo4, respectively. Immunoprecipitates of anti-hAgo4 contain proteins other than hAgo4 (shown with single and double asterisks), demonstrating undesired cross-reactivity of the antibody. The protein indicated with double asterisks was identified by mass spectrometric analysis as E1B-55kDa-associated protein. h.c., heavy chains of the antibodies used for immunoprecipitation. (*B*) Immunoprecipitates of anti-hAgo2 analyzed by Western blot analysis with anti-hAgo2. (*C*) Immunoprecipitates of anti-hAgo3 analyzed by Western blot analysis with anti-hAgo3.

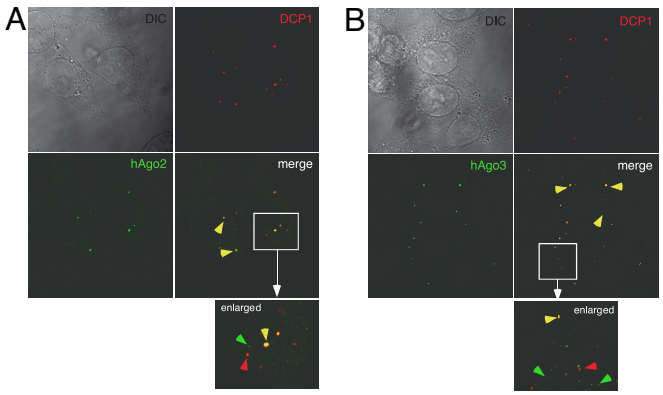


**Fig. 2.** Immunofluorescence on HeLa cells with anti-hAgo2 and anti-hAgo3. (*A*) HeLa cells immunostained with anti-hAgo2 and anti-DCP1a antibodies. It is shown that hAgo2 localizes in P-bodies (green), the cytoplasmic foci where miRNA targets are accumulated as a consequence of translational repression mediated by Argonaute–miRNA complexes (15, 16). The staining patters of hAgo2 were quite similar to those of epitope-tagged hAgo2 exogenously expressed in HEK 293 or U2-OS cells (10, 11, 13). Almost all of the P-bodies, where DCP1a, a factor functioning in mRNA decay in the bodies (17), resides (red), are costained with anti-hAgo2 (yellow arrowheads in merged image). Part of the merged image is enlarged (enlarged), where a P-body costained with anti-hAgo2 and anti-DCP1a is indicated by a yellow arrowhead. We occasionally found foci only stained with anti-hAgo2 and anti-DCP1a, which are indicated by green and red arrowheads, respectively. (*B*) HeLa cells stained with anti-hAgo3 (green) and anti-DCP1a (red). Almost all of the P-bodies are stained with both of the antibodies (yellow arrowheads). The cytoplasmic foci containing only hAgo3 or DCP1a are indicated by green and red arrowheads, respectively (in the enlarged image).

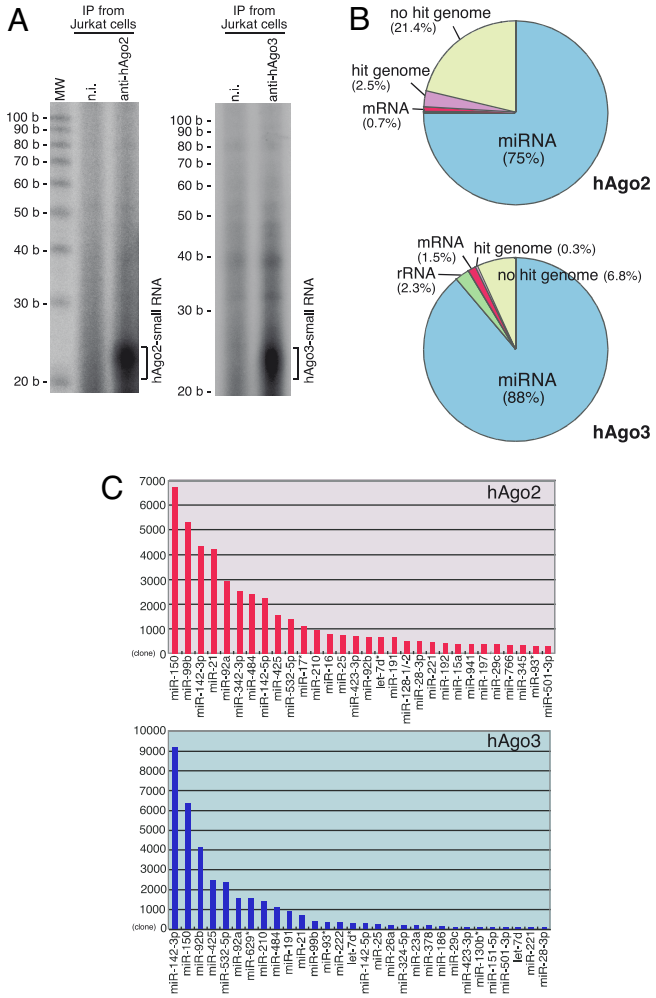


**Fig. 3.** Identification of small RNAs associated with hAgo2 and hAgo3 in Jurkat cells. (*A*) Small RNAs associated with hAgo2 and hAgo3 in Jurkat cells visualized by $^{32}$P-labeling. Both hAgos are associated with small RNAs ranging from 21 to 23 nt in length. (*B*) Compositions of small RNAs in the hAgo2 and hAgo3 libraries. The most abundant class of small RNAs in both libraries was miRNAs. Small RNAs corresponding to sequences of piRNA (piwi-interacting RNA) (0.03%), rRNA (ribosomal RNA) (0.08%), tRNA (transfer RNA) (0.004%), snRNA (small nuclear RNA) (0.002%), snoRNA (small nucleolar RNA) (0.01%), and scRNA (small cytoplasmic RNA) (0.004%) appear in the hAgo2 library. The hAgo3 library had piRNA (0.13%), tRNA (0.001%), snRNA (0.01%), snoRNA (0.005%), and scRNA (0.007%). Their appearance was negligible; thus, they apparently did not show up in the graphs. (*C*) Top 30 miRNAs appearing in each library.

obtained in the experiments was lower than that of hAgo2 small RNAs. This would have been due to the fact that hAgo3 expression levels are lower than those of hAgo2 in Jurkat cells (data not shown). Other factors, such as immunoprecipitation efficiency, could also be at play. To identify the small RNAs with hAgo2 and hAgo3, cDNA libraries were constructed and high-throughput pyrosequencing was performed. Total reads from hAgo2 and hAgo3 libraries were 68,976 and 85,690, respectively. Compositions of small RNAs identified are shown in Fig. 3*B*. It was clearly indicated that the majority in both libraries were miRNAs [≈75% (51,780) and ≈88% (76,084) in hAgo2 and hAgo3, respectively] representing 203 (hAgo2) and 181 (hAgo3) distinct known miRNAs (Dataset S1). Five novel miRNA candidates were also found in the hAgo2 library (Fig. S4).

miRNA profiles in the hAgo2 and hAgo3 libraries overlapped to a large extent. The Top 30 miRNAs in both libraries are summarized in Fig. 3*C* and Table S1. miRNAs such as miR-150 and miR-142-3p appeared frequently in both [13.0% and 16.7% (miR-150) and 8.4% and 24.2% (miR-142-3p) of total miRNAs in the hAgo2 and hAgo3 libraries, respectively] (Fig. 3*c*). We also observed that some miRNAs were discriminated by hAgo2 and hAgo3. The Top 20 miRNAs observed differentially in the hAgo2 and hAgo3 libraries are summarized in Dataset S2. Although it remains unknown how such miRNA loading discrimination occurs *in vivo*, it is suggested that hAgo2 and hAgo3 are occasionally directed to specific target mRNAs.

miRNA profiling studies have been performed in 26 different organ systems and cell types of human and rodents (18), where sequence variations in mature miRNA are reported. As well, Morin *et al.* (19) have recently reported from massively parallel sequencing that miRNAs expressed in human embryonic stem cells (hESCs) and embryoid bodies (EBs) exhibited sequence variation at their 5′ and 3′ ends. In our study, we also found end-sequence variations for nearly all of the miRNAs we identified in the hAgo2 and hAgo3 libraries (Fig. S5). 3′-Terminal additions were more apparent than 5′-terminal additions (Fig. 4). Some of these nucleotide additions likely occurred after miRNA maturation by Dicer and Drosha processing, because those nucleotides were not identical to the precursor sequences (nontemplated extensions) (Fig. 4*A*). We further examined the variations and found that the addition of A, U, and C, but little or no G addition, occurred at both ends (Fig. S6). Other variants had additional nucleotides that were identical to the precursor sequences (alternative ends) (Fig. 4*B*), indicating that they might be produced directly through Dicer and Drosha miRNA processing activities. miRNAs with alterative ends appeared more frequently than those with nontemplated extensions (Fig. 4). Although the prevalence was lower compared with that of 3′-end variations, 5′-end variations were also clearly observed. This raised the possibility that various miRNAs containing different "seed" sequences, the core region of miRNAs functioning in identifying miRNA target transcripts (20), are produced from one precursor sequence *in vivo*.

**Endogenous hAgo2 Slicer Activity.** Transfection experiments have revealed that in humans only hAgo2 has Slicer activity (10, 11). However, we wondered whether endogenous hAgo2 could indeed exhibit Slicer activity. In the transfection experiments, it was unclear whether hAgo2 was purified alone or copurified with other hAgos. In our case, immunopurified hAgo2 in an Empigen buffer did not copurify with other hAgos (Fig. S3) but still associated with miRNAs (Fig. 3). hAgo2 immunopurified from HeLa cells under presumably milder Nonidet P-40 conditions was able to cleave a target RNA containing a sequence completely matching to miR-21 (miR-21 target) (Fig. 5*A*). We also observed that hAgo2 immunopurified from HeLa cells in an Empigen buffer was able to exhibit Slicer activity (Fig. 5*A*). When isolated in Empigen, hAgo2 showed less activity to bind with miR-21 and to cleave the target than itself isolated in Nonidet P-40 (Fig. 5 *A* and *B*). This was most likely due to Empigen's affecting the strength of the antibody to bind the antigen (data not shown).

**Endogenous hAgo3 Does Not Function as Slicer.** We assessed whether endogenous hAgo3 shows Slicer activity like endogenous hAgo2. The appearance of miR-150 in the hAgo2 and hAgo3 libraries was 13.0% and 16.7%, respectively (Fig. 3*C*). Thus, *in vitro* target RNA cleavage assays were set up to target RNA (miR-150 target) harboring a sequence fully complementary to miR-150. hAgo3 was immunopurified from three volumes of the Jurkat cell lysate that was used for hAgo2 immunopurification; the amount of hAgo3 immunopurified was ≈78% of that of hAgo2 (Fig. S7). Northern blot analysis confirmed that the amounts of miR-150 associated with hAgo3 under such

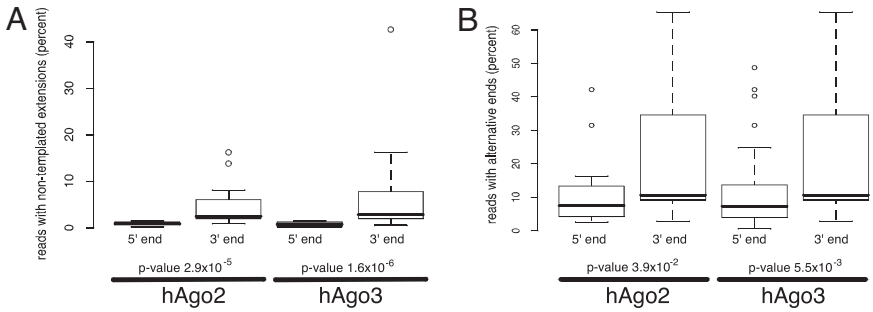


**Fig. 4.** Occurrence of variations at the 5′ and 3′ ends of miRNA with hAgo2 and hAgo3. (*A*) Occurrence of nontemplated extensions at the 5′ and 3′ ends of miRNA compared for hAgo2 and hAgo3. The Wilcoxon matched-pair signed-rank test was used to test for any significant difference between nontemplated extensions occurring at 5′ and 3′ ends. There is a significant difference between the occurrence of nontemplated extensions at 5′ and 3′ in both hAgo2 ($P \leq 2.9 \times 10^{-5}$) and hAgo3 ($P \leq 1.6 \times 10^{-6}$). The blank square represents the interquartile range (IQR) of the first quartile (Q1) and third quartile (Q3) where 50% of the observed points are included. The thick horizontal line drawn in the square represents the median of the distribution. The lower whisker represents Q1 − 1.5 × IQR, whereas the upper whisker represents Q3 + 1.5 × IQR. Observations outside of the whiskers are ''outliers,'' represented as white circles. (*B*) Occurrences of alternative ends at 5′ and 3′ ends compared for hAgo2 and hAgo3. There are significant differences between the occurrence of alternative ends at 5′ and 3′ in both hAgo2 ($P \leq 3.9 \times 10^{-2}$) and hAgo3 ($P \leq 5.5 \times 10^{-3}$).

circumstances were approximately half of that bound to hAgo2 (Fig. S7). Nonetheless, we found that hAgo3 immunopurified from Jurkat cells showed little or no Slicer activity (Fig. 5*C*). We then examined whether hAgo3 cleaves target RNA when associated with siRNA. hAgo3 bound with *luc* guide siRNA was subjected to target RNA cleavage assays for a *luc* RNA target. Cleavage activity was not observed for hAgo3 (Fig. 5*D*), although single-stranded *luc* guide siRNA was loaded onto hAgo3 to the same extent as on hAgo2 (Fig. 5*E*).

**Functional Significance of 5′-End Variations.** Ago2 cleaves its cognate RNA target across from nucleotides 10 and 11, measured from the 5′ end of the guide small RNA (21). Thus, if a miRNA had variants with an extension of one or two nucleotides at the 5′ end, the hAgo2-miRNA-mediated cleavage should give rise to two or more cleaved products that differed in size. We found that miR-142-5p has one very abundant variant with a CC addition at the 5′ end (Fig. S5). Thus, *in vitro* target RNA cleavage assays with a target harboring a sequence completely complementary to miR-142-5p (miR-142-5p target) was performed. The target was predominantly cleaved at two major sites; one corresponding to the site of the cleavage directed by registered miR-142-5p, and the other corresponding to the site of the cleavage directed by one very abundant miR-142-5p variant that had two additional nucleotides (mostly CC) at the 5′ end (miR-142-5p+CC; Fig. S8). miR-142-5p target modified with a methyl group at the expected cleavage site by miR-142-5p+CC showed strong resistance to miR-142-5p+CC but not to registered miR-142-5p cleavage (Fig. S8). Our data clearly indicated that miRNA variants with a 5′ extension existed *in vivo* and that miRNAs that have variants can at least exhibit slightly different target specificities.

## Discussion

From our experience, especially from studies on *Drosophila* RNA silencing mechanisms, we were aware that producing and using specific antibodies against individual Argonautes was an effective means to understand their functional contributions in RNA silencing (22–24). In this study, to gain a better insight into the functions of human endogenous Argonautes in RNA silencing, we produced monoclonal antibodies against each member and carried out various experiments. Anti-hAgo1 and -hAgo4 worked for Western blot analysis but showed inefficiencies in immunoprecipitation. Anti-hAgo2 and anti-hAgo3 worked quite efficiently for immunoprecipitation, even under the harsh conditions that were intentionally selected to avoid undesired protein–protein interactions that are presumed to occur *in vivo*. Through the experiments, we found that (*i*) endogenous hAgo2 and hAgo3 in Jurkat cells associate with various kinds of miRNAs, and that (*ii*) endogenous hAgo3 most likely does not function as Slicer, as opposed to hAgo2. The anti-hAgo2 and -hAgo3 antibodies we raised were very versatile and revealed that hAgo2 and hAgo3 localize in P-bodies. miRNA targets are accumulated to P-bodies as a consequence of translational repression for being finally degraded or stored until the mRNAs are once again pulled back to the cytoplasm to be translated (16). Our findings indicated that endogenous hAgo3 functions in a translational repression pathway mediated by miRNAs. The hAgo3–siRNA complex showed little or no Slicer activity. This new finding regarding endogenous hAgo3 raised two possibilities in human RNAi: (*i*) hAgo3 antagonizes RNAi activity, whereas hAgo2 functions as Slicer in RNAi *in vivo*; and (*ii*) siRNA loading onto hAgo3 apparently requires other protein(s) that need to unwind siRNA duplex before loading single-stranded siRNA. It has previously been shown that hAgo2 Slicer activity is closely involved in the siRNA duplex unwinding process in mammalian RNAi (25, 26).

miRNAs associated with hAgo2 and hAgo3 overlapped to a large extent. However, some seemed to be discriminately loaded onto either hAgo2 or hAgo3. It is reported that in *Caenorhabditis elegans*, structural features of small RNA precursors determine Argonaute loading (27). In this study, such structural discrimination in regard to miRNA loading was not observed, although comprehensive analysis remains to be performed. It has been shown that the reduced levels of miR-24 are observed in mAgo2$^{-/-}$ MEF (mouse embryo fibroblast) cells but not in mAgo3$^{-/-}$ MEF cells, suggesting that mAgo1, mAgo3, and mAgo4 do not compensate for the loss of mAgo2 activity (28). Here, we found that in Jurkat cells, albeit at a very low rate (0.21%), miR-24 was observed only with hAgo2 but did not appear at all with hAgo3. Thus, it may be possible that miR-24 is unloaded onto mAgo3 even in mice, and that it must be the reason that loss of mAgo3 did not affect the miR-24 levels in MEFs. mAgo2 has been shown as essential for RNAi in MEFs. It has also been shown that MEFs lacking mAgo2 were devoid of RNAi activity although mAgo3 was likely expressed normally in the particular cells (10). It is possible that Ago3 also has no Slicer activity in mice, as in humans. How some miRNAs are loaded onto specific hAgos remains an open question. However, a regulatory mechanism may be involved in regulating the expression levels of individual miRNAs in different cell types and tissues, where the levels of hAgos themselves may likewise be specified by unknown mechanisms.

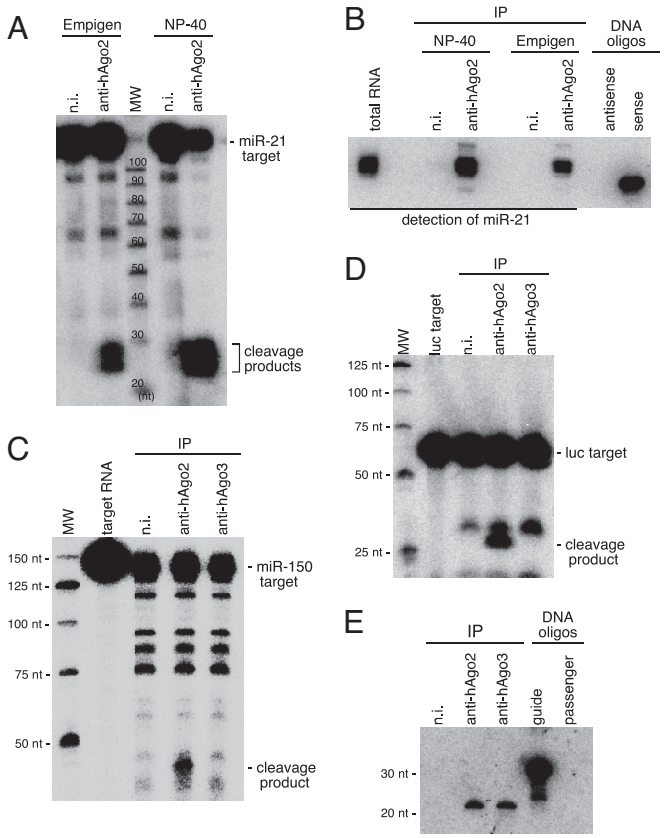


**Fig. 5.** Endogenous hAgo2 and hAgo3 Slicer activities. (*A*) Immunopurified hAgo2 from HeLa cells, which contained miR-21 (shown in *B*), subjected to *in vitro* target RNA cleavage assays. Even hAgo2 immunopurified from HeLa cells in an Empigen buffer shows Slicer activity. (*B*) miR-21 associated with hAgo2 in HeLa cell lysates prepared in a buffer containing Nonidet P-40 or Empigen visualized by Northern blot analysis. Total RNAs from HeLa cells and DNA oligos with sequences of miR-21 (sense) and miR-21* (antisense) were used as controls. (*C*) Immunopurified hAgo2 and hAgo3 from Jurkat cells in an Empigen buffer were subjected to *in vitro* target RNA cleavage assays. hAgo3 does not cleave a target RNA (miR-150 target), whereas hAgo2 does. Association of hAgo3 with miR-150 is confirmed by Northern blot analysis (Fig. S7*B*). (*D*) hAgo2 and hAgo3 associated with *luc* guide siRNA subjected to *in vitro* target RNA cleavage assays. hAgo2 but not hAgo3 cleaves the *luc* target RNA. (*E*) Northern blot analysis showing that hAgo2 and hAgo3 are able to be loaded with *luc* guide siRNA under the same circumstances.

miRNA sequence variations have been observed in humans and rodents (18). In the study, the A and U additions at the 3′ ends were discovered. Morin *et al.* (19) have recently revealed that there are variations at the 5′ and 3′ ends of miRNAs expressed in hESCs and EBs. In this study, we also found that miRNAs associated with hAgo2 and hAgo3 showed various variations at the 5′ and 3′ ends. We found the 5′-end variations quite interesting, because they presumably alter miRNA abilities with respect to recognizing targets *in vivo*. In miRNA sequences, the second to eighth nucleotides from the 5′ ends are called "seed" sequences, and the regions function in defining miRNA targets in the miRNA pathway (20). Sequence variations at the 5′ ends mean that these miRNA variants, although produced from the same precursor sequence, might recognize a different set of target sequences from those of the miRNAs first registered in the databases. Indeed, in this study we showed by *in vitro* target RNA cleavage assays that miRNA variants with a 5′ extension existed *in vivo*, and that miRNAs that have variants can at least exhibit slightly different target specificities.

The accumulation of data on endogenous Argonautes and other crucial factors in RNA silencing, including triggering small RNA molecules, will contribute to a comprehensive understanding of RNAi and other RNA silencing mechanisms. Our study clearly indicated that the hAgo antibodies we raised are tools that can accurately reveal the functional behavior of Argonautes and their miRNA partners in RNA silencing. Thus, they can potentially provide us with valuable information about how physiological and biological aspects of our lives are regulated through such mechanisms.

## Methods

**Production of Monoclonal Antibodies.** The N termini of hAgo1, hAgo2, hAgo3, and hAgo4 (accession nos. NM_012199, NM_012154, NM_024852, and NM_017629) (171, 148, 175, and 164 aa from the N-terminal ends of hAgo1, hAgo2, hAgo3, and hAgo4, respectively) were fused either with GST (hAgo1 and hAgo2) or 6× His-tag (hAgo3 and hAgo4). Each of the fusion proteins was produced in and purified from *Escherichia coli* and used as an antigen to immunize mice. Anti-hAgo monoclonal antibodies were produced essentially as described in ref. 24. Western blot analysis was performed essentially as described in ref. 24.

**Immunofluorescence.** Immunofluorescence was performed essentially as described in ref. 29. After fixation, cell permeabilization was carried out with 0.1% Triton X-100 containing PBS, instead of cold acetone. Anti-DCP1a was used at 1:400 dilution. Anti-hAgo2 and -hAgo3 used were culture supernatants of the hybridomas. Alexa Fluor 488-conjugated anti-mouse IgG and Alexa Fluor 546-conjugated anti-rabbit IgG (Molecular Probes) were used as secondary antibodies to detect anti-hAgos and anti-DCP1a, respectively. All images were obtained by using a Zeiss LSM510 laser scanning microscope.

**Immunoprecipitation.** Immunoprecipitation was performed from HeLa and Jurkat cells. Cell lysis buffer with Nonidet P-40 contained 30 mM Hepes-KOH (pH 7.3), 150 mM KOAc, 2 mM MgOAc, 5 mM DTT, 0.1% Nonidet P-40, 2 $\mu$g/ml pepstatin, 2 $\mu$g/ml leupeptin, and 0.5% aprotinin. Empigen-containing cell lysis buffer was 1× PBS containing 1 mM EDTA, 0.1 mM DTT, 1% Empigen (Calbiochem), 2 $\mu$g/ml pepstatin, 2 $\mu$g/ml leupeptin, and 0.5% aprotinin. After immunoprecipitation, total RNAs were isolated from the immunoprecipitates with phenol:chloroform and precipitated with ethanol. RNAs were dephosphorylated with CIP (NEB) and labeled with [$\gamma$-$^{32}$P]ATP with T4 polynucleotide kinase (Takara) for visualization. Silver staining was performed by using a SilverQuest kit (Invitrogen).

**Small RNA Library Construction.** Cloning of small RNAs associated with hAgo2 and hAgo3 was carried out essentially as described in ref. 24, using a DynaExpress miRNA cloning kit (BioDynamics Laboratory). First-strand cDNA synthesis was performed with Reverse Transcriptase (BioDynamics Laboratory). PCR was performed with Ex Taq polymerase (Takara) first and then KOD plus (TOYOBO). High-throughput pyrosequencing was performed on a GS20 system (Roche). RNA sequences between 5′ and 3′ adapters were analyzed by Takara. Briefly, each of the small RNAs was located in the human genome by using the BLAT program in the UCSC Genome Browser (http://genome.ucsc.edu/cgi-bin/hgBlat) and then searched by using the National Center for Biotechnology Information BLAST (www.ncbi.nlm.nih.gov/blast) and Ensemble BlastView (www.ensembl.org/Multi/blastview) to determine matching to rRNA, tRNA, snRNA, snoRNA, and scRNA. The miRBase (http://microrna.sanger.ac.uk/sequences) was used to identify miRNA clones in humans and other species.

**Northern Blot Analysis.** Northern blot analysis was performed essentially as reported in ref. 22. Total RNAs were isolated from immunoprecipitates with phenol:chloroform and precipitated with ethanol. The probe used for miR-21 was 5′-TCAACATCAGTCTGATAAGCTA-3′. The sequence of a probe used for detecting luc guide siRNA is described in ref. 30. The DNA oligo was labeled with T4 polynucleotide kinase in the presence of [$\gamma$-$^{32}$P]ATP. Control oligos used were as follows: sense strand (miR-21), 5′-CTCAACATCAGTCTGATAAGCTAG-3′; antisense strand (miR-21), 5′-AATTCTAGCTTATCAGACTGATGTTGAGGTAC-3′; *luc* guide oligo, 5′-GAATTCTCGAAGTATTCCGCGTACGTGGGTACC-3′. First, Jurkat cell lysate was prepared as described in ref. 30, and *luc* siRNA duplex was then added to the lysate. After incubation at 37°C for 1 h, hAgo2 and hAgo3 were immunopurified by using the specific antibodies in an Empigen buffer, and guide siRNA bound to the proteins was detected by Northern blot analysis.

***In Vitro* Target RNA Cleavage Assay.** Target RNA cleavage assays using immunoprecipitates were performed in a reaction buffer containing 25 mM Hepes-KOH (pH 7.4), 50 mM KOAc, 5 mM MgOAc, 5 mM DTT, 0.1 units/ml RNasin (Promega), and 1 $\mu$g of yeast RNA (Ambion). After reaction for 3 h at 37°C, RNAs were isolated from the whole reaction mixtures, run on gels, and visualized on a BAS 2500. To make miR-21 target RNA, a set of DNA oligos (5′-CTCAACATCAGTCTGATAAGCTAG-3′ and 5′-AATTCTAGCTTATCAGACTGATGTTGAGGTAC-3′) was annealed and inserted into a pBS SKII+ vector digested with KpnI and EcoRI. To make a target for miR-150, a short DNA fragment produced by annealing a set of oligo DNAs (5′- TCGAGCACTGGTACAAGGGTTGGGAGAG-3′ and 5′-AATTCTCTCCCAACCCTTGTACCAGTGC-3′) was inserted in a pBS SKII+ vector digested with XhoI and EcoRI. PCR was performed by using primers for the T7 and T3 promoter sequences, and the PCR products were then used as templates for *in vitro* transcription with a MEGAscript T7 kit (Ambion). To make a luc target, pBS-luc-target plasmid (30) was digested with BamHI, and transcription was performed with a MEGAscript T7 kit. The resultant RNAs were radiolabeled with [$\gamma$-$^{32}$P]ATP by using T4 polynucleotide kinase and were gel-purified.

**Bioinformatics.** Small RNA sequences were aligned to miRNA precursor sequences obtained from miRBase (http://microrna.sanger.ac.uk) by our custom perl script to identify mature miRNA sequences with nontemplated bases or with alternative ends. Sequences that had more than one base mismatches to their precursors were discarded, as were sequences with $<$10 reads. We used the top 30 abundant sequences for our sequence data analysis. The most abundant sequence with perfect base matches to its precursor sequence was considered to be the canonical mature form. Other sequences with perfect base matches were considered as mature miRNA sequences with alternative ends. A mature miRNA sequence with nontemplated bases was a sequence having at its 5′- or 3′-end one mismatch with the corresponding precursor sequences.

**ACKNOWLEDGMENTS.** We thank J. Lykke-Andersen for providing the anti-DCP1a antibody; K. Saito for technical advice; T. Mori, T. N. Okada, and Y. Kawamura for technical assistance; and other members of the Siomi laboratory for discussions and comments on the manuscript. For help in MS analysis, we acknowledge I. Sagawa (University of Tokushima Faculty of Medicine Support Center for Advanced Medical Sciences). This work was supported in part by grants to M.C.S. and H.S. from the Ministry of Education, Culture, Sports, Science and Technology (Japan) and the New Energy and Industrial Technology Development Organization. M.C.S. is supported by Core Research for Evolutional Science and Technology of the Japan Science and Technology Agency. M.C.S. is Associate Professor of Global COE for Human Metabolomics Systems Biology of the Ministry of Education, Culture, Sports, Science, and Technology. H.S. is a member of the Genome Network Project.

1. Zaratiegui M, Irvine DV, Martienssen RA (2007) Noncoding RNAs and gene silencing. *Cell* 128:763–776.
2. Tomari Y, Zamore PD (2005) Perspective: Machines for RNAi. *Genes Dev* 19:517–529.
3. Kloosterman WP, Plasterk RH (2006) The diverse functions of microRNAs in animal development and disease. *Dev Cell* 11:441–450.
4. Bushati N, Cohen SM (2007) MicroRNA function. *Annu Rev Cell Dev Biol* 23:175–205.
5. Peters L, Meister G (2007) Argonaute proteins: Mediators of RNA silencing. *Mol Cell* 26:611–623.
6. O'Donnell KA, Boeke JD (2007) Mighty Piwis defend the germline against genome intruders. *Cell* 129:37–44.
7. Aravin AA, Hannon GJ, Brennecke J (2007) The Piwi-piRNA pathway provides an adaptive defense in the transposon arms race. *Science* 318:761–764.
8. Hutvagner G, Zamore PD (2002) A microRNA in a multiple-turnover RNAi enzyme complex. *Science* 297:2056–2060.
9. Mourelatos Z, *et al.* (2002) miRNPs: A novel class of ribonucleoproteins containing numerous microRNAs. *Genes Dev* 16:720–728.
10. Liu J, *et al.* (2004) Argonaute2 is the catalytic engine of mammalian RNAi. *Science* 305:1437–1441.
11. Meister G, *et al.* (2004) Human Argonaute2 mediates RNA cleavage targeted by miRNAs and siRNAs. *Mol Cell* 15:185–197.
12. Beitzinger M, Peters L, Zhu JY, Kremmer E, Meister G (2007) Identification of human microRNA targets from isolated Argonaute protein complexes. *RNA Biol* 4:e1–e9.
13. Sen GL, Blau HM (2005) Argonaute 2/RISC resides in sites of mammalian mRNA decay known as cytoplasmic bodies. *Nat Cell Biol* 7:633–636.
14. Gabler S, *et al.* (1998) E1B 55-kilodalton-associated protein: A cellular protein with RNA-binding activity implicated in nucleocytoplasmic transport of adenovirus and cellular mRNAs. *J Virol* 72:7960–7971.
15. Liu J, Valencia-Sanchez MA, Hannon GJ, Parker R (2005) MicroRNA-dependent localization of targeted mRNAs to mammalian P-bodies. *Nat Cell Biol* 7:719–723.
16. Pillai RS, *et al.* (2005) Inhibition of translational initiation by let-7 microRNA in human cells. *Science* 309:1573–1576.
17. Fenger-Gron M, Fillman C, Norrild B, Lykke-Andersen J (2005) Multiple processing body factors and the ARE binding protein TTP activate mRNA decapping. *Mol Cell* 20:905–915.
18. Landgraf P, *et al.* (2007) A mammalian microRNA expression atlas based on small RNA library sequence. *Cell* 129:1401–1414.
19. Morin RD, *et al.* (2007) Application of massively parallel sequencing to microRNA profiling and discovery in human embryonic stem cells. *Genome Res* 18:610–621.
20. Lewis BP, Shih IH, Jones-Rhoades MW, Bartel DP, Burge CB (2003) Prediction of mammalian microRNA targets. *Cell* 115:787–798.
21. Elbashir SM, Lendeckel W, Tuschl T (2001) RNA interference is mediated by 21- and 22-mucleotide RNAs. *Genes Dev* 15:188–200.
22. Saito K, *et al.* (2006) Specific association of Piwi with rasiRNAs derived from retrotransposon and heterochromatic regions in the Drosophila genome. *Genes Dev* 20:2214–2222.
23. Gunawardane LS, *et al.* (2007) A Slicer-mediated mechanism for repeat-associated siRNA 5′ end formation in Drosophila. *Science* 315:1587–1590.
24. Nishida KM, *et al.* (2007) Gene silencing mechanisms mediated by Aubergine-piRNA complexes in Drosophila male gonad. *RNA* 13:1911–1922.
25. Matranga C, Tomari Y, Shin C, Bartel DP, Zamore PD (2005) Passenger-strand cleavage facilitates assembly of siRNA into Ago2-containing RNAi enzyme complexes. *Cell* 123:607–620.
26. Leuschner PJ, Ameres SL, Kueng S, Martinez J (2006) Cleavage of the siRNA passenger strand during RISC assembly in human cells. *EMBO Rep* 7:314–320.
27. Steiner FA, *et al.* (2007) Structural features of small RNA precursors determine Argonaute loading in Caenorhabditis elegans. *Nat Struct Mol Biol* 14:927–933.
28. O'Carroll D, *et al.* (2007) A Slicer-independent role for Argonaute 2 in hematopoiesis and the microRNA pathway. *Genes Dev* 21:1999–2004.
29. Siomi H, Dreyfuss G (1995) A nuclear localization domain in the hnRNP A1 protein. *J Cell Biol* 129:551–560.
30. Miyoshi K, Tsukumo H, Nagami T, Siomi H, Siomi MC (2005) Slicer function of Drosophila Argonautes and its involvement in RISC formation. *Genes Dev* 19:2837–2848.